Dynamic behaviours of piston rings and their practical impact. Part 2: oil transport, friction and wear of ring/liner interface and the effects of piston and ring dynamics

T Tian
Sloan Automotive Laboratory, Massachusetts Institute of Technology, 60 Vassar Street, Building 31-166, Cambridge, MA 02139, USA

Abstract: The paper discusses several important processes that have great impact on the lubrication between the top two rings and the liner. The analysis is conducted on the basis of the calculation results on a heavy-duty (HD) diesel engine using theoretical models. Oil supply mechanisms to different liner regions are analysed, and emphasis is given to the oil transport to the top liner region that is found critical to friction, wear and oil consumption in HD diesel engines. Additionally, the paper discusses the oil supply to the second ring, its uncertainties and the effect on the prediction of the performance of the top two rings. Furthermore, the effects of dynamics of the piston and rings on friction, wear and oil transport are illustrated and the effects of bore distortion on oil transport are discussed.

For practical purposes, a formula to describe the second ring running surface profile is given based on simple geometrical constraint. A new truncation method is rendered for plateau surface roughness in order to effectively use the existing mixed lubrication models.

Keywords: dynamic behaviours, piston rings, oil transport, friction, wear

NOTATION

ATDC	above top dead centre
BDC	bottom dead centre
DIN	Deutsches Institut für Normung
FMEP	friction mean effective pressure
HD	heavy duty
ID	inner diameter location of the ring–groove contact
LOFT	liner oil-film thickness
MOFT	minimum oil-film thickness
OCR	oil control ring
OD	outer diameter location of the ring–groove contact
OS1	first oil supply mechanism discussed in the paper, namely there is sufficient oil supply to the second ring during down-strokes
OS2	second oil supply mechanism discussed in the paper, namely oil supply to the second ring during down-strokes only comes from the oil control ring
P	contact pressure
TDC	top dead centre
TLOCR	twin-land oil control ring
TPOCR	three-piece oil control ring
UOCR	ulfex oil control ring
V	ring sliding speed

The MS was received on 1 November 2001 and was accepted after revision for publication on 11 March 2002.

1 THE LUBRICATION CONDITIONS OF TOP TWO RINGS

Two critical factors that affect the lubrication of the top two rings are oil availability and the effects of gas pressure. These two factors are largely controlled by the dynamics of the rings and the piston, which determine the location of the minimum point on the running surface of the rings. In this paper, discussions are based on the calculations using a computer model [**1**, **2**] on a

heavy-duty (HD) diesel engine. An HD diesel engine was chosen as it presents severe lubrication conditions due to its high pressure, high temperature and low speed.

The computer model has been improved to take into account the effects of ring dynamic twist, bore expansion and piston dynamic tilt. Specifically, the model considers the change in the relative profile between the ring running surface and the liner due to the change in the angles of ring dynamic twist, bore expansion and piston dynamics as well as the oil squeezing effects due to the rate of change in these angles. The effects of the piston dynamic tilt is treated in a pseudo-three-dimensional manner such that the relative angle between the ring neutral plane and the liner, α_{rl} is represented as

$$\alpha_{rl} = \alpha_{tw} + \alpha_{pt} \cos \theta + \alpha_{be} \quad (1)$$

where α_{tw} is the ring dynamic twist angle that is assumed to be uniform along the circumference and is obtained from a ring dynamics and gas flow model [**1**, **3**–**5**], α_{pt} is the piston dynamic tilt, θ is the angle representing the circumferential location of the ring section interested and α_{be} is the liner tilt angle due to bore expansion (Fig. 1).

The lubrication condition and the minimum oil-film thickness (MOFT) of the top two rings are shown in Figs 2 and 3 respectively. A brief description of engine and rings is shown in Fig. 4. Figure 5 plots the piston tilt data used for the calculation. The sign convention in Fig. 5 is that the positive value represents the piston's top tilting to the minor thrust side. It needs to be noted that the piston tilt trace in Fig. 5 is not from this engine. However, the piston tilt in Fig. 5 represents the general trend of the secondary motion of mono-pistons, namely the piston tilts towards the minor thrust side at the end of the compression stroke and shifts to the major thrust side in the early part of the expansion stroke, and it is sufficient for the illustration purpose of this paper.

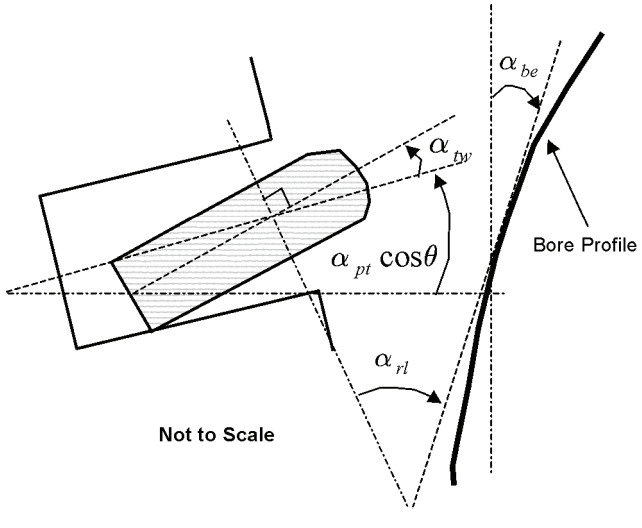

Fig. 1 Angles of ring twist, piston tilt and bore expansion

In each plot in Fig. 2, two solid curves represent the upper and lower bounds of the wetting region between the ring running surface and the liner, and the dot-dashed curve represents the location of the minimum point. When the three lines merge into one, hydrodynamic lubrication disappears and only boundary lubrication exists. The results are based on an assumption that there is sufficient oil supplying the second ring from the liner during downstrokes when the second ring travels below the liner location where the oil control ring (OCR) is at TDC. This assumption sets an upper limit on the amount of the oil supply to the top two rings. Further discussions on the mechanisms of the oil supply to the top two rings in different liner regions will be given later in the paper.

Above the TDC location of the OCR, the film thickness on the liner is assumed to be zero at the beginning of the calculation and all the results shown in Figs 2 and 3 are those after 10 cycles of calculation when the lubrication condition of the top two rings obtains cycle–cycle convergence. As sufficient oil supply is assumed below the TDC location of the OCR, only possible cycle–cycle variation during the first few cycles exists when a ring travels in the liner region between the TDC location of the top ring and the TDC location of the OCR, to be referred to as the *'dry' region*. The horizontal dotted lines in Fig. 2 are the edges of the running surface of the rings and the upper edge of the second ring is not included in the figure, as it is not affecting the discussions.

In Fig. 3, the horizontal dotted line in each plot represents a height of four times of the r.m.s. value of the combined roughness between the rings and liner, and thus there is asperity contact if the MOFT is below this line according to the asperity contact model used [**6**, **7**]. It can thus immediately be seen that both rings experience boundary lubrication over a significant portion of the cycle and the lubrication condition of the top ring becomes extremely severe around the TDC of the compression stroke due to high cylinder pressure (close to 200 bar), low sliding speed and little or zero oil available. Slight ring collapse occurs during second ring flutter [**5**] in the late part of the compression stroke and the early part of the expansion stroke and it causes the sudden jumps in the MOFT of the second ring in Fig. 3.

To assist the analysis of the lubrication conditions of the top ring further, the available oil-film thickness on the liner to lubricate the top ring is plotted in Fig. 6a and the volume (per unit length in the circumferential direction) of the oil between the top ring and the liner, in which the hydrodynamic pressure is generated, is plotted in Fig. 6b. Additionally, the period when the top ring travels in the 'dry' region is indicated in Fig. 6. It is worthwhile to mention that during a downstroke, below the TDC location of the second ring, the oil available to the top ring is what is left by the second ring and, above that location, the oil available to the top ring is what is left by the top ring during the previous upstroke; during

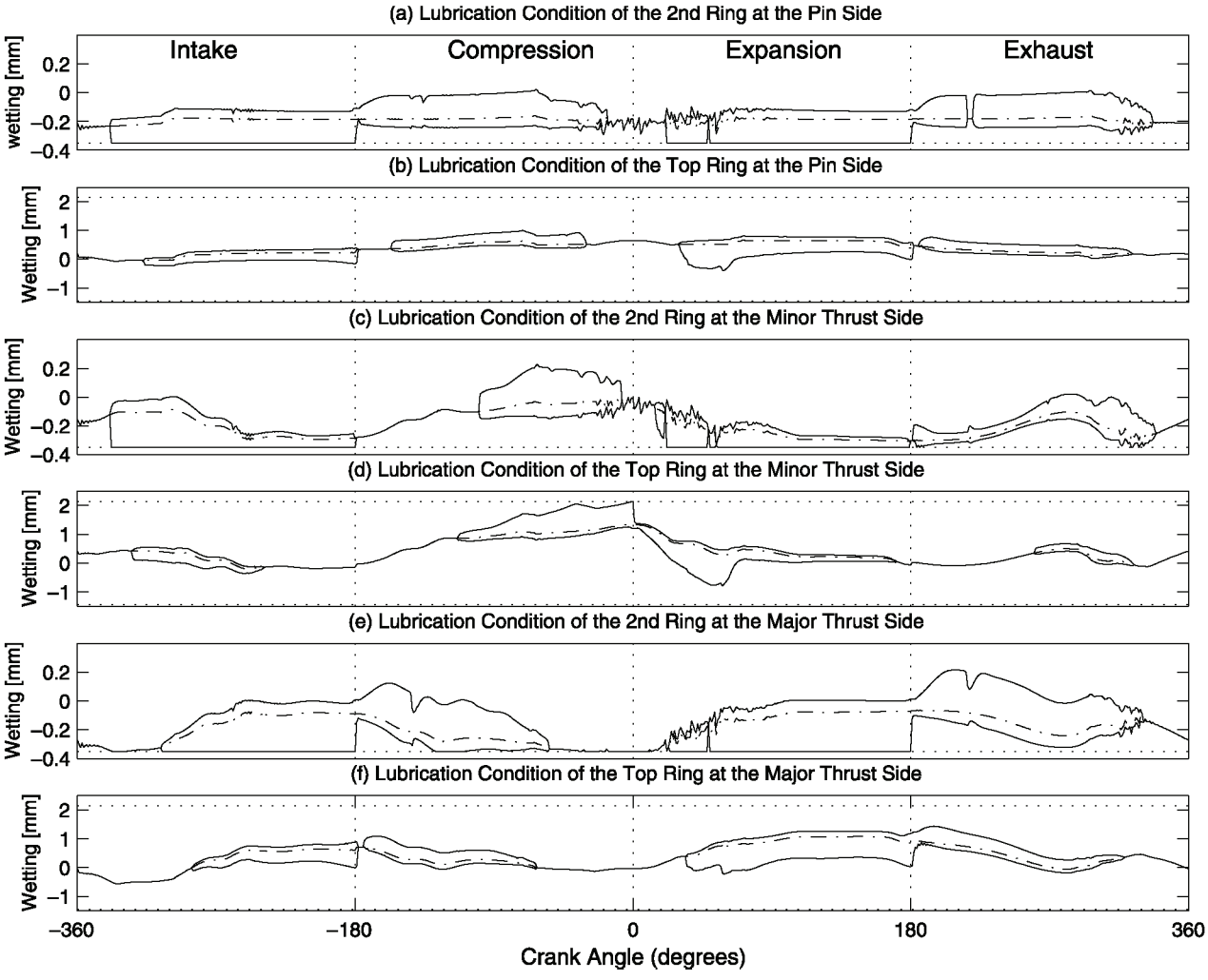

Fig. 2 The lubrication condition of the top two rings at three sections

an upstroke, the oil available to the top ring is what is left by the top ring during the previous downstroke.

The piston dynamic tilt causes the variation in the location of the minimum point and thus the converging width on the running surface of second ring along the circumference. Comparing the results of pin, major and minor sides in Figs 2 and 6, it can clearly be seen that the smaller converging width (length between the dot-dashed curve and the lower solid curve in Figs 2a, c and e) of the second ring during a downstroke results in less available oil and less MOFT for the top ring when the top ring travels outside the 'dry' region. In this particular case, the dynamic twist of the second ring is not significant. Therefore, the variation in the converging width of the second ring and thus the oil supply to the top ring are mainly affected by the piston dynamic tilt.

2 OIL TRANSPORT IN THE 'DRY' REGION

The oil available to the top ring (a result of the second ring lubrication) has profound effects on the oil supply to the 'dry' region and the lubrication of the top ring in the 'dry' region. As shown in Fig. 2c, at the minor thrust side, the relatively large converging width of the second ring at the beginning of the intake stroke results in a high oil-film thickness on the liner available to the top ring (Fig. 6a). This high oil-film thickness in the region just outside the 'dry' region is not significantly changed by the passage of the top ring that follows the second ring in the intake stroke because the top ring is not scraping oil on the liner (Fig. 2d). As a result, this high oil-film thickness just outside the 'dry' region is still available to the top ring when it comes back to this region during the compression stroke, which can be clearly seen in Fig. 6a where the film thickness trace before the 'dry' region in the compression stroke is almost a mirror image of that just after the 'dry' region in the intake stroke. Because of this high available oil-film thickness, the wetting width (Fig. 2d) and the oil volume (Fig. 6b) of the wetted region of the top ring increase before the top ring enters the 'dry' region during the compression stroke at the minor thrust side. Then, when the top ring enters the 'dry' region, it starts

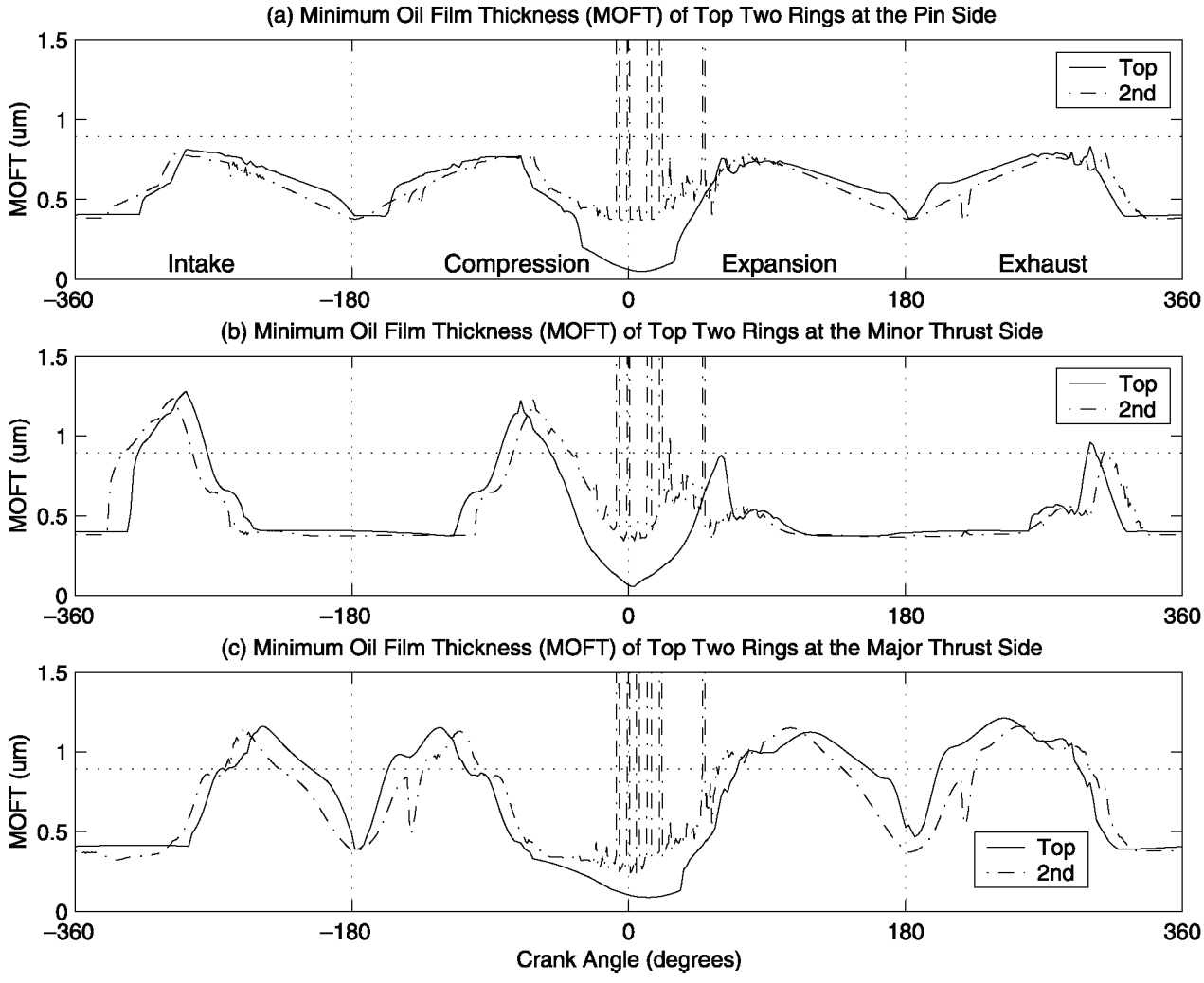

Fig. 3 MOFT of the top two rings at three sections

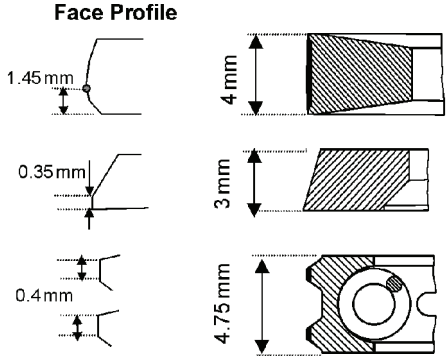

Engine Displacement Volume: 2Liter/cylinder
Operating Condition: 1200rpm/full-load
Peak cylinder pressure: 187 bars
Roughness (Rq): Liner = 0.2μm, Rings = 0.1μm
Liner Temperature: TDC: 160°C; BDC 137 °C
Oil: 10W50

Fig. 4 Brief description of rings, engine and operating condition (TDC, top dead centre; BDC, bottom dead centre)

to release the accumulated oil to the 'dry' region and is able to keep the 'dry' region wetted. Conversely, at the pin and major thrust sides, the top ring is not able to wet the 'dry' region, as there is not sufficient oil accumulation before it enters the 'dry' region. There is another important factor that causes the increase in oil accumulation between ring and the liner before the top ring enters the 'dry' region during the compression stroke at the minor thrust side. During the late part of the compression stroke, the piston tilts towards the minor thrust side. Thus, the location of the minimum point of the top ring running surface (Fig. 2d) is the highest of all the circumferential locations. As a result, the radial load increase due to gas pressure is the most at the minor thrust side. An increase in the radial load tends to make the top ring hold more oil in order to create more hydrodynamic pressure.

As pointed out in references [**1**] and [**2**], the existence of oil in the 'dry' region is due to the balance between the amount of the oil brought into the 'dry' region by

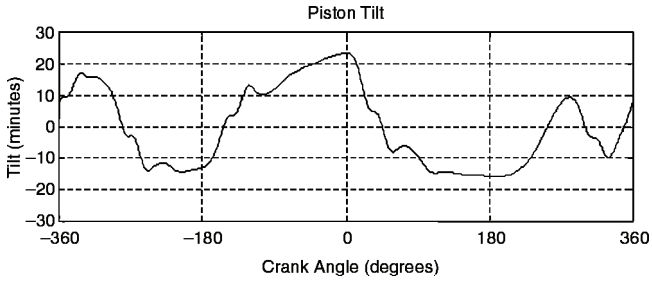

Fig. 5 Piston tilt used for the calculations

the top ring during the compression stroke and the oil carried away during the expansion stroke. Figure 7 shows the LOFT before and after the passage of the top ring for the pin and minor thrust sides. The results in Fig. 7 are from the second cycle of the calculation. It can be seen from Fig. 7b that, at the minor thrust side, the top ring is able to wet a larger area during the compression stroke than the previous cycle as the non-zero oil-film thickness region is advanced from −18° to −10°. Moreover, during the expansion stroke, not all the extra oil that moved into the 'dry' region during the compression stroke is carried away. As a result, a larger area in the 'dry' region is wetted after the passage of the top ring in the second cycle. In fact, after 3 cycles, the 'dry' region is fully wetted and the top ring gains hydrodynamic lubrication in the 'dry' region during the compression and expansion strokes.

Conversely, at the pin side (Fig. 7a), a balance is almost reached between the amount of the oil brought into the 'dry' region by the top ring during the compression stroke and carried away during the expansion stroke. Therefore, the top ring is never able to bring oil further into the 'dry' region. On the other hand, it was found that on the pin side the top ring is able to maintain the 'dry' region wetted if a certain amount of the oil-film thickness is 'placed' in the 'dry' region at the beginning of the calculation; this was also found in references [**1**] and [**2**] where the piston tilt was not considered. Nonetheless, in the following discussion, the pin side is considered to be not fully wetted.

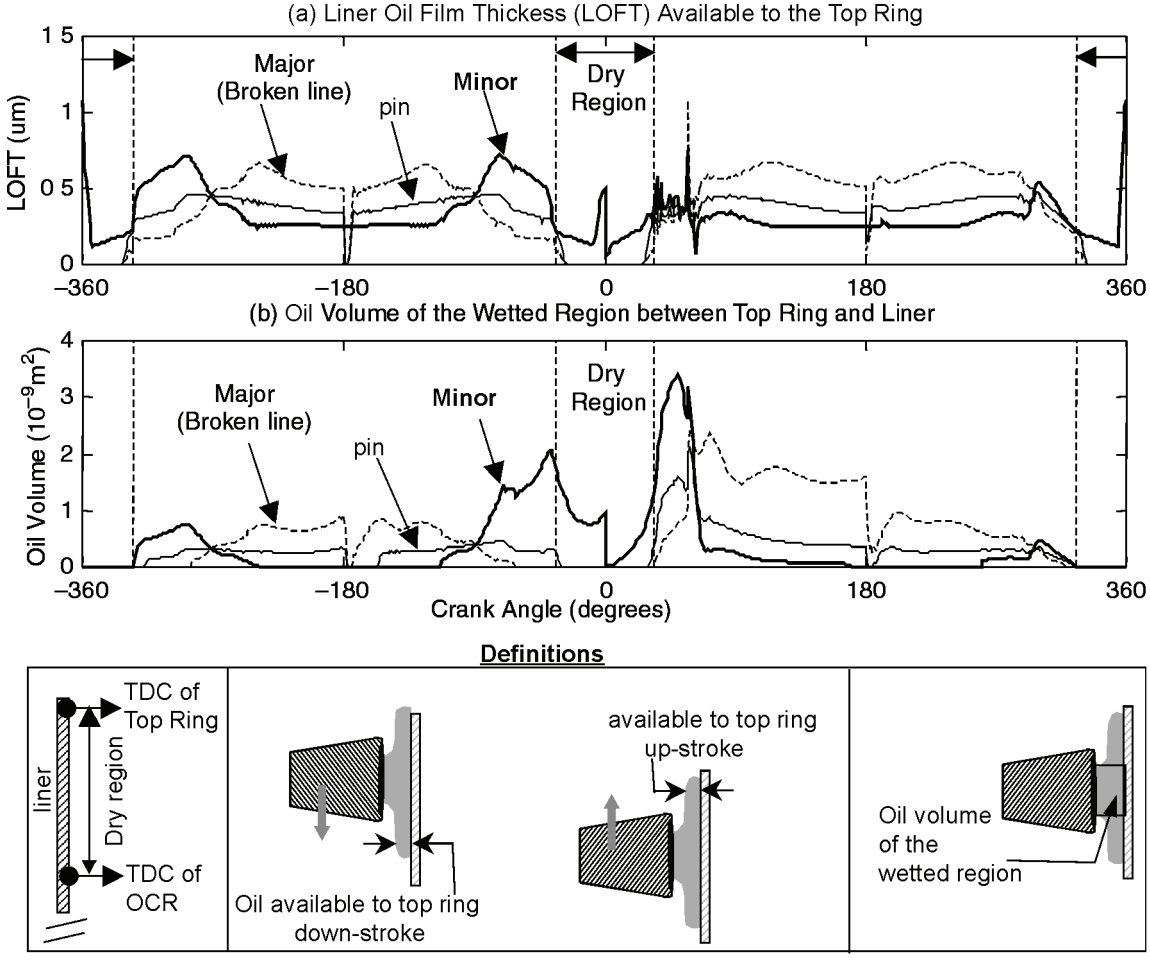

Fig. 6 Oil available on the liner to the top ring and oil volume held by the top ring (LOFT, liner oil-film thickness)

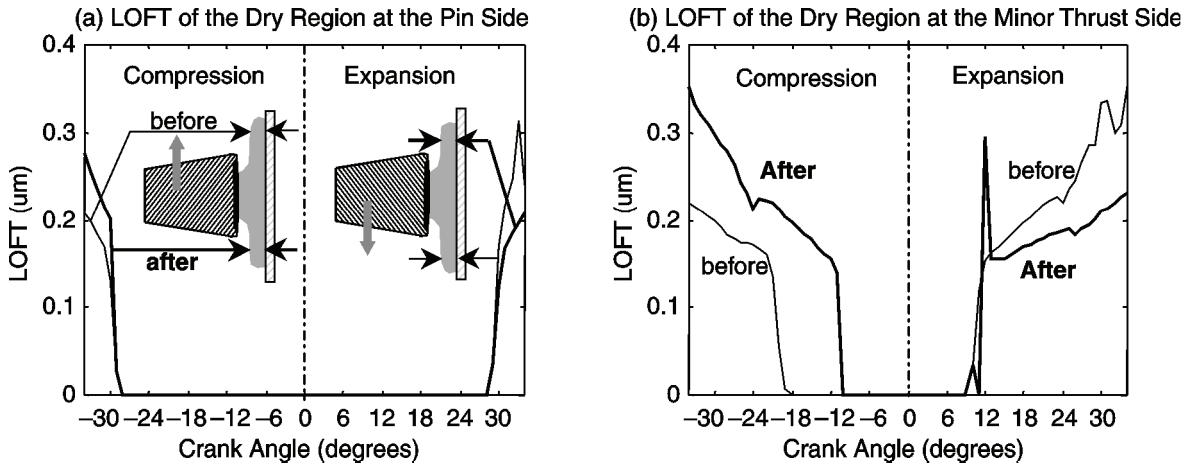

Fig. 7 Comparison of oil transport to the 'dry' region between two sections: results of the second cycle of the calculation

All these analyses are intended to demonstrate the main point that the capability of the top ring to carry the oil into the 'dry' region mainly depends on the availability of oil to the top ring before it enters the 'dry' region during the compression stroke. For this particular case studied, it seems that, at or around the minor thrust side, the top ring is able to bring sufficient oil into the 'dry' region and to gain hydrodynamic lubrication mainly because a relatively high oil-film thickness passes the second ring during the early part of the intake stroke and the oil was virtually 'untouched' after the passage of the top ring during the intake stroke. Additionally, a critical assumption here is that there is sufficient oil supply to the second ring during downstrokes. Therefore, for any other different cases, changes in piston tilt in the intake stroke and oil availability to the second ring can cause differences in the results. As will be discussed later, if the assumption on the availability of oil to the second ring goes to the other extreme, the 'dry' region can never be wetted through the oil transport of the ring/liner interface.

Nonetheless, from a theoretical point of view, it is difficult to bring the oil to the 'dry' region and to lubricate the top ring at all the circumferential locations if the ring/liner interface is the only oil source. Certainly, oil on the second land and crown land, if there is sufficient accumulation, can flow to the 'dry' region. For HD diesel engines, the length of the 'dry' region is significant and the top ring spends an appreciable amount of time in the 'dry' region. Insufficient oil in the 'dry' region can have significant adverse effects on wear; friction and excessive wear of the 'dry' region in the liner can cause problems in blowby and oil consumption [**8**]. On the other hand, excessive oil available to the top ring before it enters the 'dry' region can make the top ring scrape the oil on the liner before it enters the 'dry' region during the compression stroke and can cause problems in oil consumption, as will be discussed later.

3 OIL SUPPLY MECHANISMS TO THE SECOND RING AND SCRAPING BY THE SECOND RING

The results presented earlier are based on the assumption that there is sufficient oil supply to the second ring during downstrokes and this assumption [i.e. the first oil supply mechanism (OS1)] sets up an upper limit in terms of oil supply to the top two rings from the liner. A direct implication of this assumption is that the lubrication of the top two rings is independent of the performance of the OCR. There exists sufficient experimental evidence that shows a large amount of oil in the third land [**9–13**] in both diesel and gasoline engines. On the other hand, it is common sense that the tension of the OCR has a great impact on oil consumption and top ring lubrication. Therefore, the real situation is that the oil supply to the second ring/liner interface during downstrokes may come from both the OCR/liner interface and the third land. Fully resolving the oil supply to the second ring/liner interface apparently needs understanding of the oil transport process in the third land. Recent work by Thirouard [**9**] discovered and modelled important elements governing the oil transport in the third land. However, implementing all the mechanisms governing the oil transport in the third land in a quantitative way still needs further theoretical work and experimental verifications. Here, in order to show the difference in ring–liner lubrication that may exist due to different oil transport rate from the third land to second ring/liner interface, it is interesting to analyse the results under the other extreme condition in the oil supply to the second ring, namely, assuming that the oil supply to the second

ring during the downstrokes only comes from the OCR/liner interface [i.e. the second oil supply mechanism (OS2)].

A pseudo-three-dimensional twin-land oil control (TLOCR) model [**14**] was used to calculate the oil-film thickness left on the liner from the OCR. This model couples the dynamics of the OCR inside the groove and the ring–liner lubrication. Additionally, the effects of piston tilt are considered in the model. For a large TLOCR such as that in the HD diesel engine (Fig. 4), the piston tilt has predominant effects in controlling the oil leakage through the upper land of the TLOCR.

Figures 8 and 9 show the lubrication condition and the MOFT respectively of the top two rings. The effects of less oil supply to the second ring on the wetting extent of each ring and the MOFT can be immediately seen. Except for the period when the second ring has radial collapse, asperity contact and boundary lubrication exist over the entire cycle for both rings. Additionally, the top ring is never able to bring sufficient oil to wet the 'dry' region fully and the top ring experiences pure boundary lubrication in most of the 'dry' region in the compression and expansion strokes. Furthermore, at all three sections shown in Fig. 8, in a large portion of downstrokes, the second ring's leading edge does not become fully flooded (lower edge of the second ring running surface is indicated as dot-dashed curves in Figs 8a, c, and e) due to insufficient oil supply from the TLOCR.

It has been pointed out that the piston third land has a large amount of oil accumulation [**9–13**]. The accumulation comes from many sources and one of those sources is the scraping by the second ring during downstrokes. Second ring scraping was clearly identified by Thirouard [**9**] from both experimental observation and theoretical studies using the same models as in this paper. It is thus interesting to examine the scraping by the second ring in this engine. To do this, the LOFT along the liner before and after the passage of the second ring during the intake and expansion strokes is shown in Fig. 10. The LOFT before the passage of the second ring is the oil-film thickness left by the TLOCR. The axis of

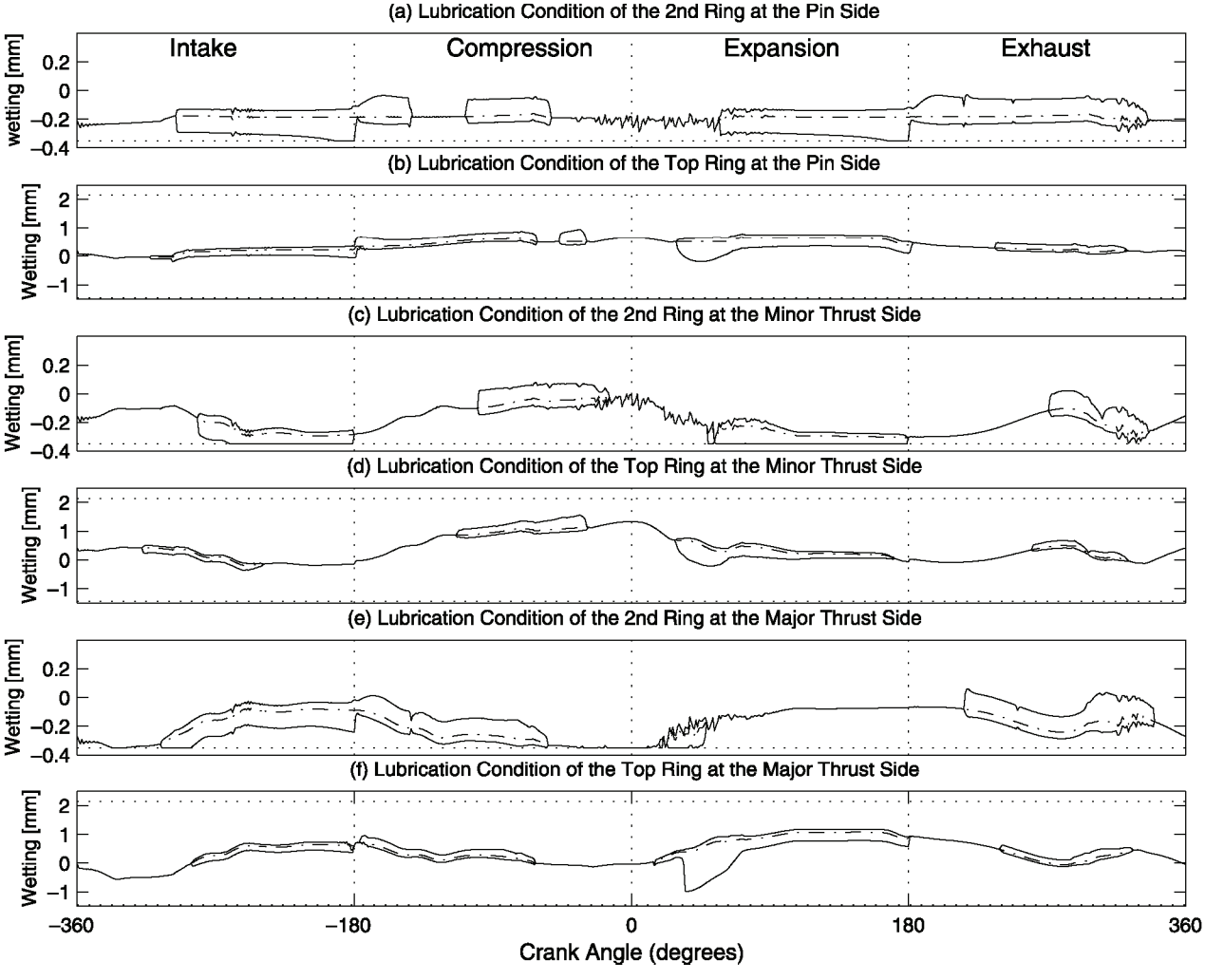

Fig. 8 Lubrication condition of the top two rings with OS2

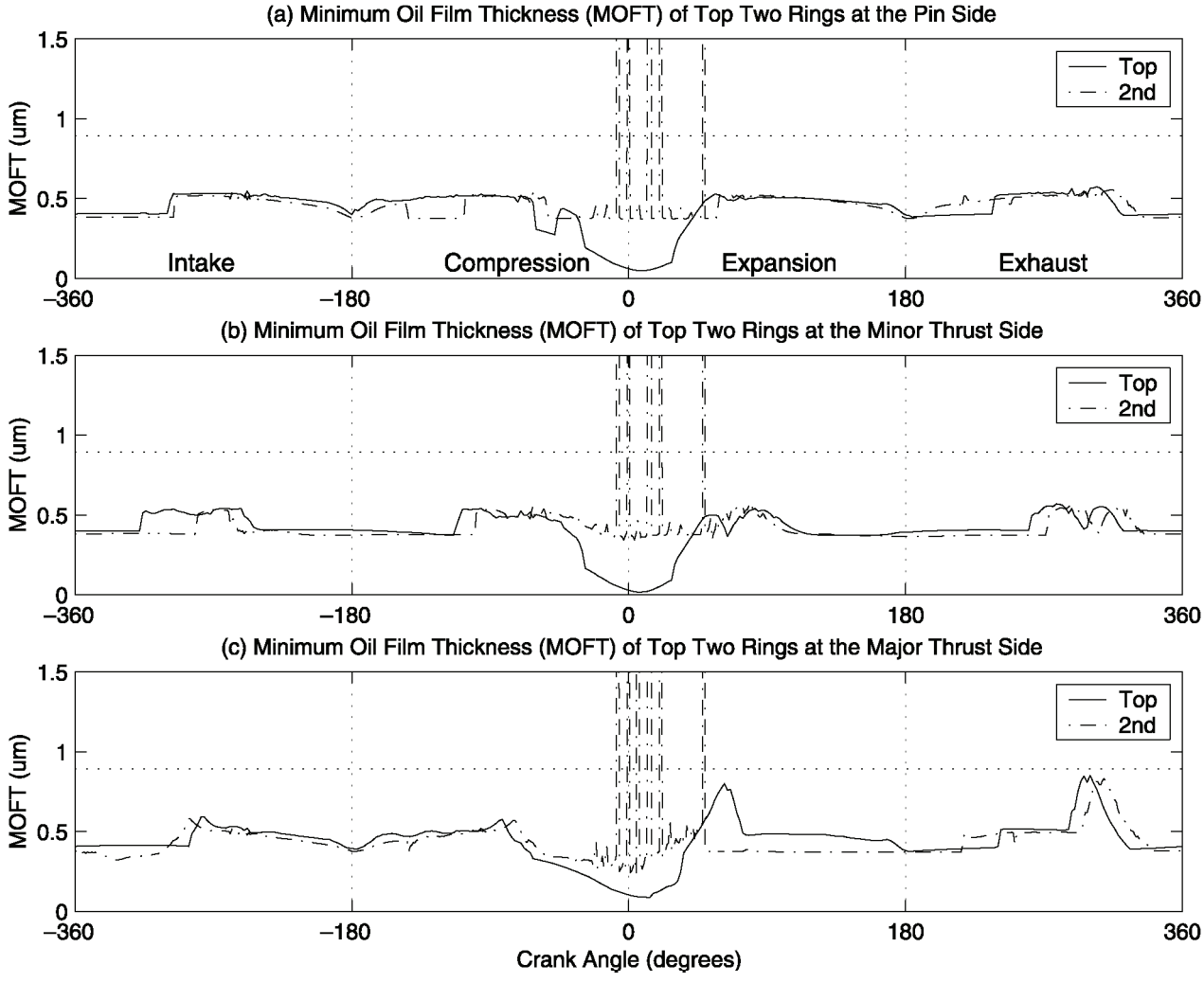

Fig. 9 MOFT of the top two rings with OS2

the liner location originates from the TDC location of the centre-line of the top ring and the plots in Fig. 10 show only the results below the TDC location of the OCR.

At the pin side (Figs 10a and b), a very small amount of the oil passes through the TLOCR because the piston tilt does not affect lubrication of the TLOCR [**14**] and the tension of the TLOCR is very high. Then, the second ring simply 'slides' through at the pin side and the oil-film left by the TLOCR is almost 'untouched' during both strokes. At both major and minor thrust sides, during some periods, the TLOCR leaves a relatively large amount of oil on the liner due to the effect of piston dynamic tilt and stiffness of the large TLOCR. As a result, scraping occurs with the second ring during these periods. Indeed, if a TLOCR is used as the OCR, the scraping by the second ring may always occur at both major and minor thrust sides due to geometrical constraints. As shown in Fig. 11, a large amount of oil leakage through the upper land of the TLOCR can only occur when the piston's top tilts away from the liner. With such a piston tilt, the minimum point of the second ring moves down along the running surface and thus the converging width of the second ring is reduced. As a result, the second ring allows less oil to pass and scraping can occur. It is thus implied that a combination of a second ring and a TLOCR forms a perfect barrier in controlling the oil leakage through the ring/liner interface. The oil control ability of the second ring can be clearly seen in Figs 9 and 10 where the MOFT of the top two rings is fairly uniform at the three circumferential locations (Fig. 9) despite the fact that the oil-film thickness left by the OCR is very non-uniform (Fig. 10). Consequently, it may be concluded that any large amount of oil that passes through the second ring/liner interface can only come from two sources:

(a) the oil supply from the third land to the second ring/liner interface and
(b) excessive oil passing the second ring due to poor conformability of the oil control ring and second ring to a distorted bore.

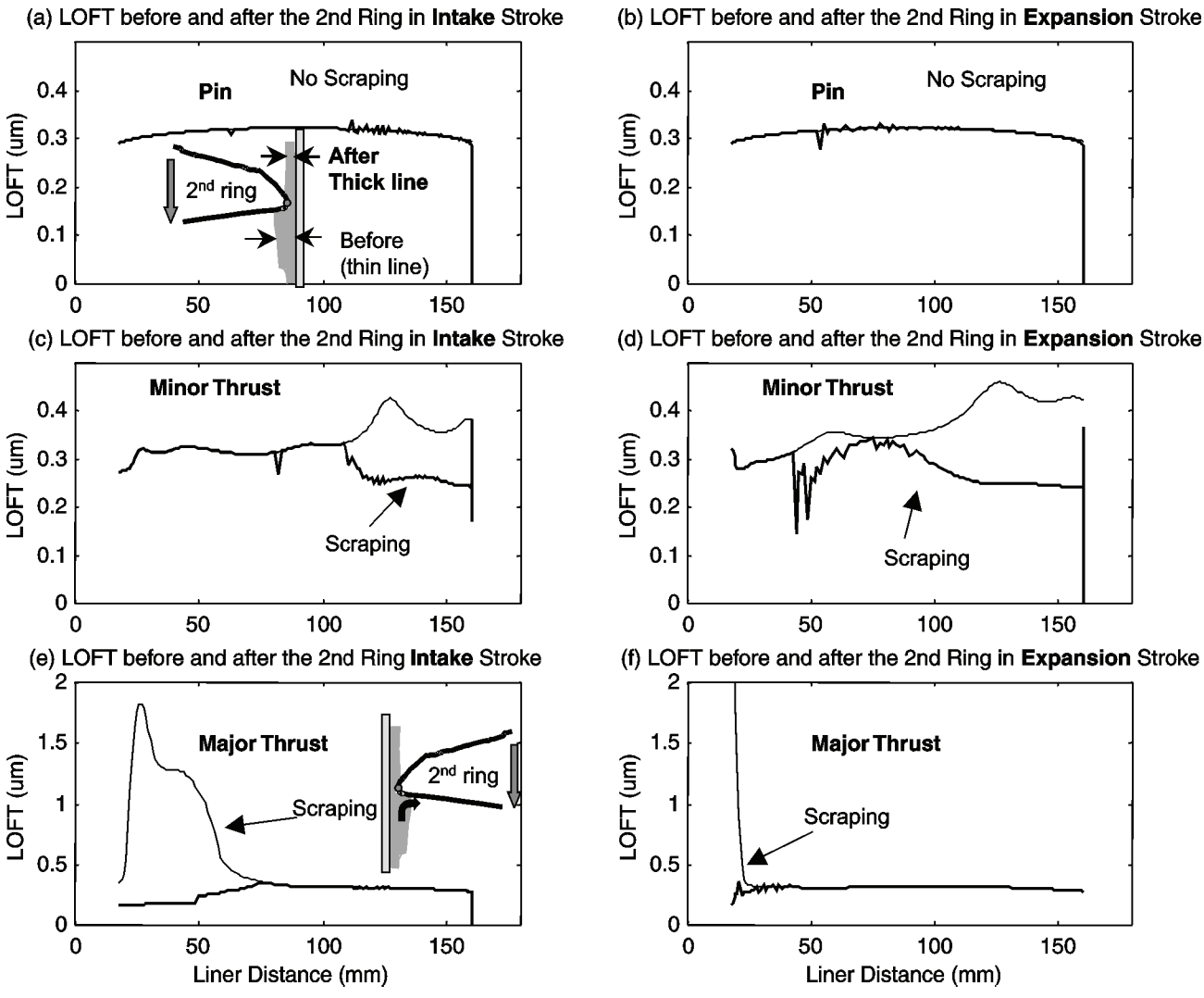

Fig. 10 Oil transport by the second ring at three sections (OS2)

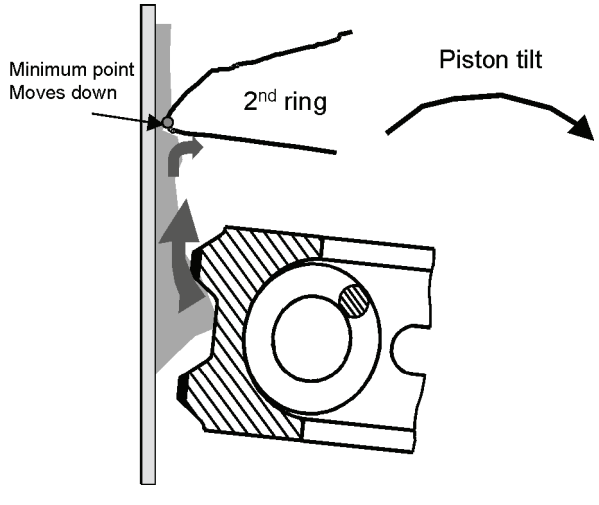

Fig. 11 Illustration of second ring scraping

For practical purposes, it is interesting to elaborate further the down-scraping function of the taper face second ring. It may be safe to state that the down-scraping of the second ring only occurs if the upper land of a TLOCR cannot conform well to the liner in the axial direction due to its high torsional stiffness and large piston tilt. A three-piece oil control ring (TPOCR) or an Ulfex oil control ring (UOCR) [**15**] does not have the same conforming problem in the axial direction due to piston tilt as a TLOCR. Therefore, second ring down-scraping may never occur for a ring pack with a TPOCR or a UOCR as the OCR. Furthermore, if bore distortion becomes significant, the second ring may not be able to control the excessive oil that passes any types of OCR because OCRs have much better conformability in the circumferential direction than a second ring due to the higher tension and small radial width of the OCR.

4 EFFECTS OF BORE DISTORTION ON OIL TRANSPORT

Bore distortion or out-of-roundness is generally considered to have adverse effects on oil consumption. From a theoretical point of view, the mechanism that could be mainly responsible for the extra oil consumption caused by bore distortion is top-ring scraping under a high cylinder pressure during the late part of compression stroke. When bore distortion becomes so large that a large oil-film thickness can pass the OCR during the intake stroke, the following second ring and top ring are not able to scrape down the oil on the liner during the intake stroke because of their poorer conformability than the OCR. Thus, the large oil-film thickness stays on the liner and can be scraped up by the top ring during the compression stroke due to the increased conformability of the top ring by the cylinder pressure that penetrates into the top-ring groove. Again, the timing is very critical. The cylinder pressure needs to be sufficiently high before the top ring enters the 'dry' region in order for the top ring to scrape up the oil on the liner. Furthermore, although some of the scraped oil may return to the liner, the rest of the oil has a great chance of being consumed by various mechanisms, causing oil consumption.

To illustrate the effects of bore distortion using this pseudo-three-dimensional model, ring tensions of all three rings are arbitrarily reduced to 25 per cent of the original values to simulate partially the regions where the rings are not conforming well to the bore. Oil supply to the second ring during downstrokes is assumed to be from the TLOCR only (OS2), i.e. minimum oil supply to the second ring.

Figure 12 shows the wetting condition and oil-film thickness left on the liner during the intake stroke for the second ring and during the compression stroke for the top ring. The liner location is used instead of crank angle and only the results outside the 'dry' region are displayed. It can be seen from Fig. 12c that the oil-film thickness left by the TLOCR is significantly increased compared with the results with the original ring tension (Fig. 10) and the oil-film left by the TLOCR just outside the 'dry' region is not affected by the passage of the top two rings during the intake stroke. When the top ring comes back during the compression stroke, scraping occurs just outside the 'dry' region since the upper edge of the top-ring running surface becomes fully flooded (Fig. 12b) and the oil-film on the liner is reduced after the passage of the top ring (Fig. 12d).

5 FRICTION, WEAR, AND OIL TRANSPORT BETWEEN THE TOP RING AND LINER AND THE EFFECTS OF RING DYNAMICS

5.1 Friction

The friction mean effective pressures (FMEP) of different rings and different mechanisms are shown in Fig. 13a. The results are the integration of five equally spaced circumferential locations from minor to major

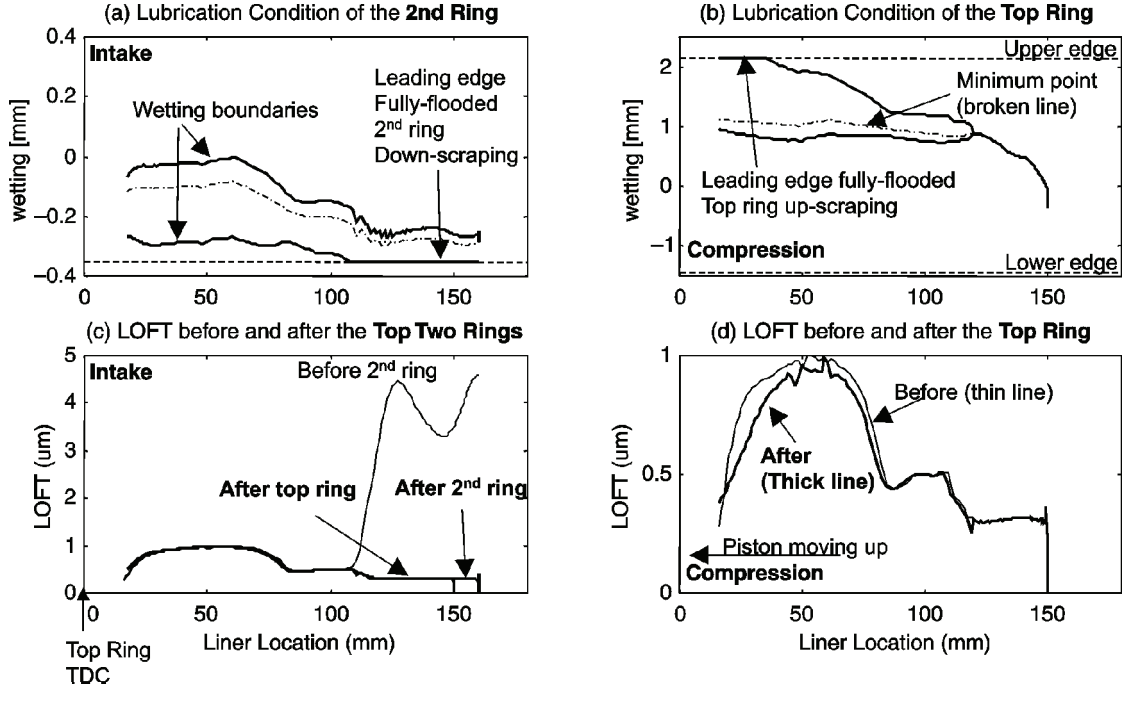

Fig. 12 Oil transport of the top two rings with reduced ring tension

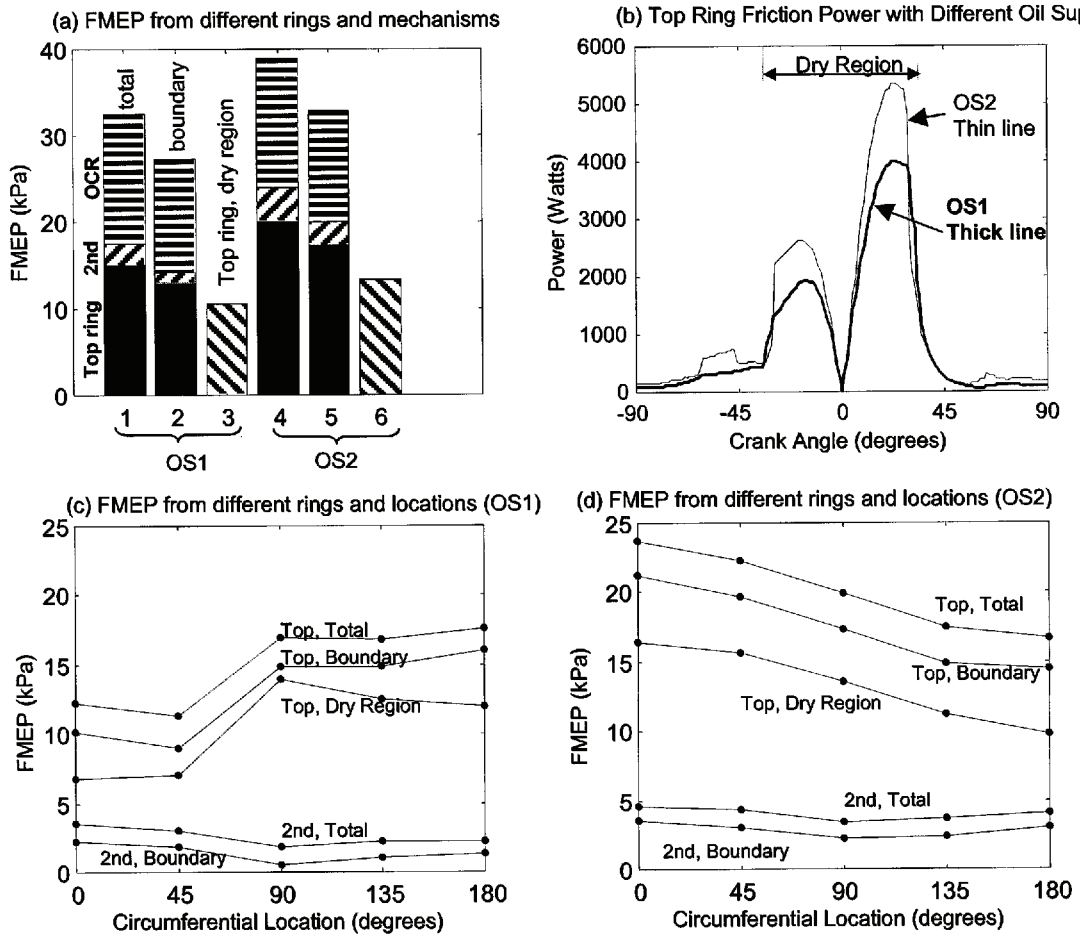

Fig. 13 Friction loss and contribution of different mechanisms, rings and sections

thrust sides. In Fig. 13a, label 1 shows the FMEPs of the top ring (bottom), second ring (middle) and the TLOCR (top), label 2 is the FMEP of the three rings from boundary lubrication only, and label 3 is the contribution of the top ring when it travels in the 'dry' region. Labels 1, 2 and 3 are the results based on the assumption that there is sufficient oil supply to the second ring during downstrokes (OS1). Labels 4, 5 and 6 are the results based on the assumption that the oil supply to the second ring during downstrokes comes only from the TLOCR/liner interface (OS2). These two different oil supply mechanisms set up lower (OS1) and upper (OS2) limits for the estimation of FMEP from the ring pack.

For both oil supply mechanisms, the FMEP is dominated by the boundary lubrication contribution. Additionally, despite the fact that it has much less tension than the OCR, the top ring contributes to the total FMEP at the same level as the OCR due to the effects of high cylinder pressure and insufficient oil supply. Furthermore, the major part of the top-ring friction power is generated when the top ring travels in the 'dry' region, which can be clearly seen in Fig. 13b.

Figures 13c and d show the FMEPs from the five circumferential locations (0° is the minor thrust side) for OS1 and OS2 respectively. For easier comparison, the integrated friction work from each circumferential location is projected to the entire bore to obtain the FMEP values in Figs 13c and d. The importance of oil supply to the top two rings can be immediately seen by comparing the results of Figs 13c and d. With sufficient oil supply to the second ring (OS1), the 'dry' region is wetted at the minor thrust side (0° and 45°) and the friction power is drastically reduced compared with the case with TLOCR as the sole oil supplier to the top two rings (OS2).

5.2 Asperity contact between the top ring and the liner and implications on wear

Asperity contact between the top ring and the liner is plotted in Fig. 14 at three circumferential locations with OS1 as the oil supply mechanism. Because of piston tilt, along the circumference the contact pressure peaks occur at different locations on the ring running surface.

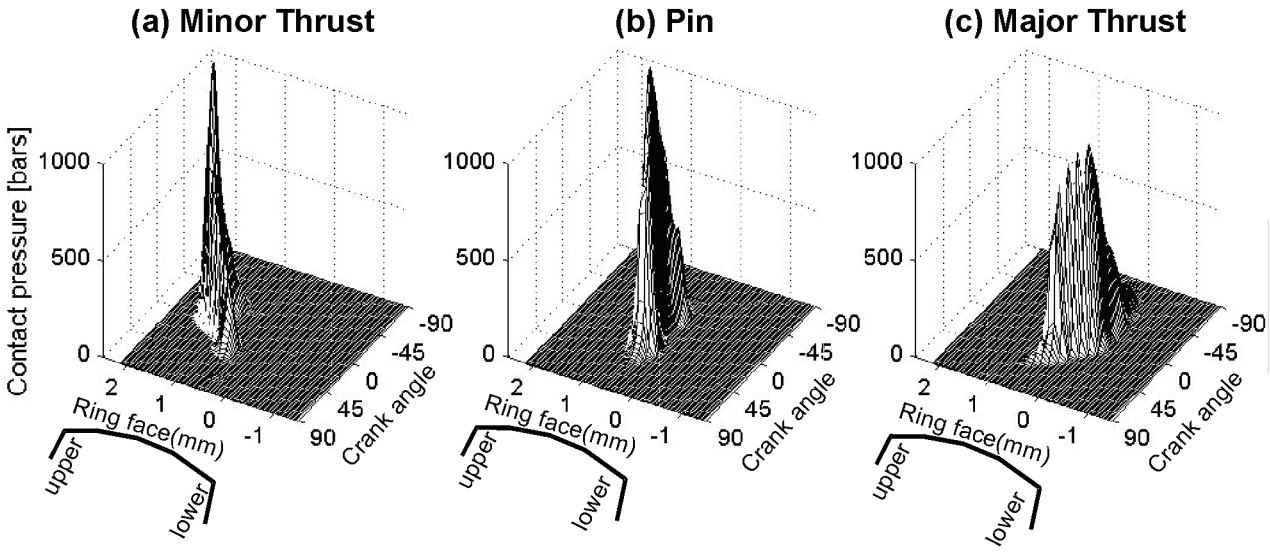

Fig. 14 Contact pressure between the top ring and liner at three sections

Although at the minor thrust side, the top ring gains hydrodynamic lubrication, the peak contact pressure is still the highest because the minimum point of the running surface is located at the highest position and the radial load due to the cylinder pressure is thus the highest before the piston slap occurs.

One way to examine the wear rate is to evaluate the product PV of the contact pressure P and travel velocity V. Figure 15 shows the averaged PV over a cycle at three positions. Again, the peak PV occurs at different locations on the running surface due to the piston tilt effects. The peak value of the averaged PV is the highest at the pin side simply because the contact location at the other two sides spreads out over the running surface due to the piston tilt. In reality, the top ring rotates. Thus, wear of any section of the ring running surface is an integrated result of all probable circumferential locations that this section passes. Here, no further attempts are made to evaluate the evolution of the worn profile of the top-ring running surface.

In order to show the difference in PV values due to different oil supply mechanisms, Fig. 16 is used to show the comparison of the averaged PV of the top ring at the minor thrust side between OS1 and OS2. The minor thrust side is chosen because the lubrication of the top ring is most affected at the minor thrust side by the oil supply mechanism, as shown in Figs 2 and 8. The drastic increase in the averaged PV due to lack of oil supply at the minor thrust side can be seen.

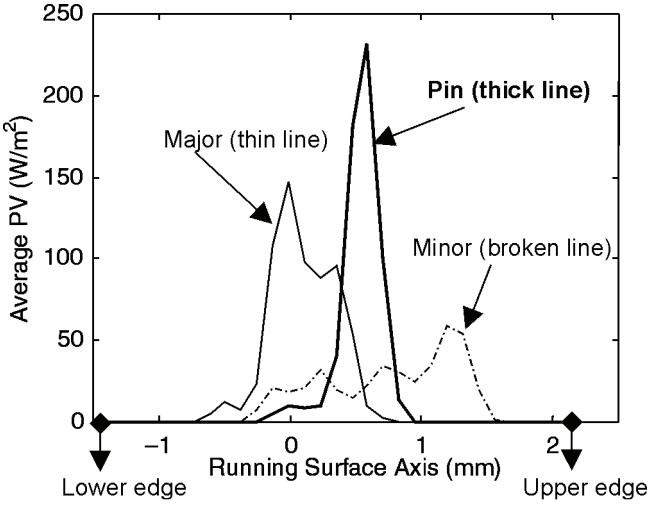

Fig. 15 Average PV at three sections

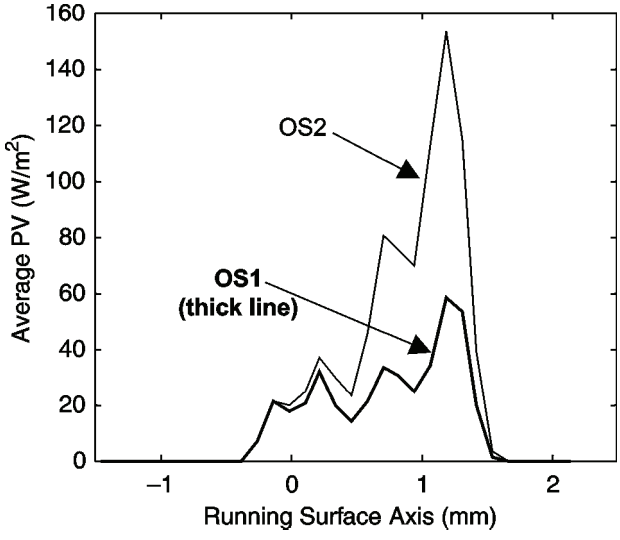

Fig. 16 Comparison of average PV at the minor thrust side between two different oil supply mechanisms

5.3 Effects of ring dynamics, groove tilt angle and face profiles

Increased radial loading due to cylinder pressure is one of the main reasons for severe top-ring–liner contact and large contribution of the top ring to the total friction power of the ring pack. The radial loading due to cylinder pressure largely depends on the location of the minimum point. Changing the minimum point of the ring running surface when the cylinder pressure is high can be realized by changing the tilt angle of the lower flank of the top-ring groove and the profile of the running surface. Groove tilt angle controls the location of the minimum point because the top ring approximately conforms to the lower side of the groove under a high cylinder pressure no matter what the static relative angle is between the lower side of the top ring and the groove [**16**].

Figure 17b shows the comparison of the averaged *PV* at the pin side between the original groove tilt used for the previous discussion and a groove tilt with 0.15° more downward tilt. It can be seen that the magnitude of the averaged *PV* is increased with more downward tilt and the location of the peak *PV* is moved up. The FMEP of the top ring is increased from 15 to 16.4 kPa. A similar effect can be seen in Fig. 17a with a symmetrical face profile; the FMEP is increased to 19 kPa. All the comparisons in Fig. 17 are based on the OS1 assumption. Furthermore, as the minimum point is moved up with increased groove downward tilt and a symmetrical profile, the top ring can scrape the oil on the liner during the compression stroke before it enters the 'dry' region (Fig. 18).

Clearly, a design that brings up the minimum point of the top ring during the period of the cycle when the cylinder pressure is high may cause adverse effects on wear, friction loss and oil consumption. Thus the minimum point of the top ring needs to be lowered, for example, by increasing the upward tilt of the groove and offsetting the barrel face. However, the ring groove and the ring running surface both experience wear during the engine's lifetime. Hence, optimizing the design needs to consider the evolution of the geometry due to wear. As will be demonstrated in the following, increasing upward tilt and offsetting the barrel face downwards may accelerate the wear of the outer diameter (OD) of the lower groove and the benefit of the initial design may vanish quickly.

Figure 19 shows the contact pressure between the lower side of the top ring and groove. The result is based on the original design parameter with an offset barrel face. The static relative angle between the lower side of the top ring and groove is positive [inner diameter (ID) seal] after the downward groove tilt due to thermal deformation is considered. It can be seen that, when the cylinder pressure rises, the contact pressure peak moves from the ID to OD due to ring dynamic twist. Governing mechanisms for the wear of the groove and ring flanks are not entirely clear. Traditional *PV* analysis was used by Piao and Gulwadi [**17**] by considering the piston secondary motion. In reference [**16**], it was found that the contact pressure distribution along the radial direction during the period of high cylinder pressure might be a good indicator for the groove wear. Here, in order to simplify the analysis, the average contact pressure between the TDC of the expansion stroke and 30° ATDC is used as an indicator of the wear between the flanks of the top ring and groove.

Figure 20 shows the averaged contact pressure between the lower flanks of the top ring and groove with a reduced downward tilt (0.1° or less), original

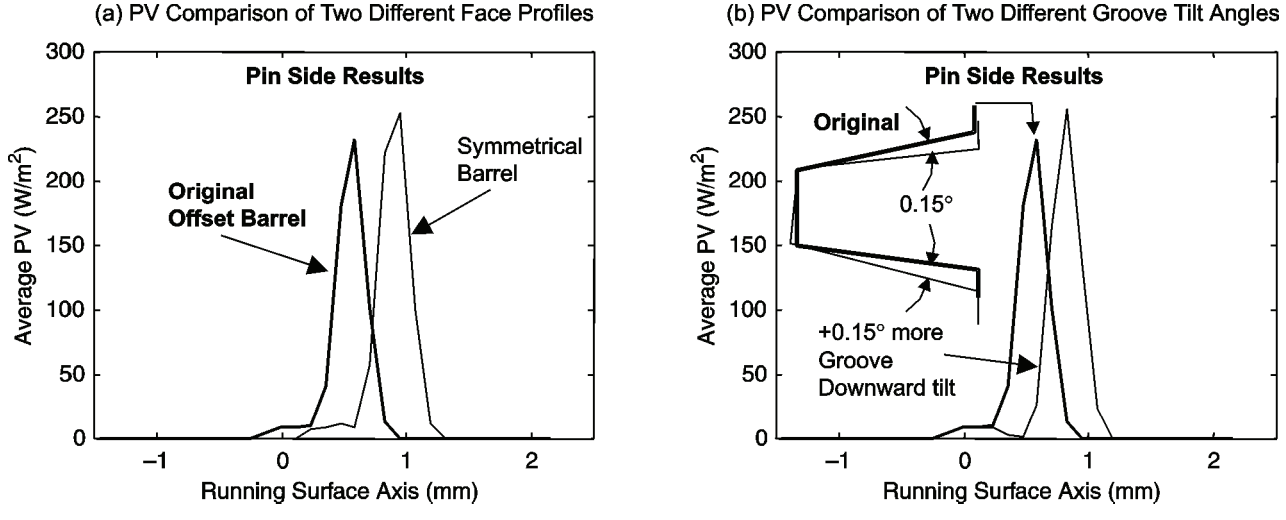

Fig. 17 Effect of groove tilt angle and face profile on average *PV*

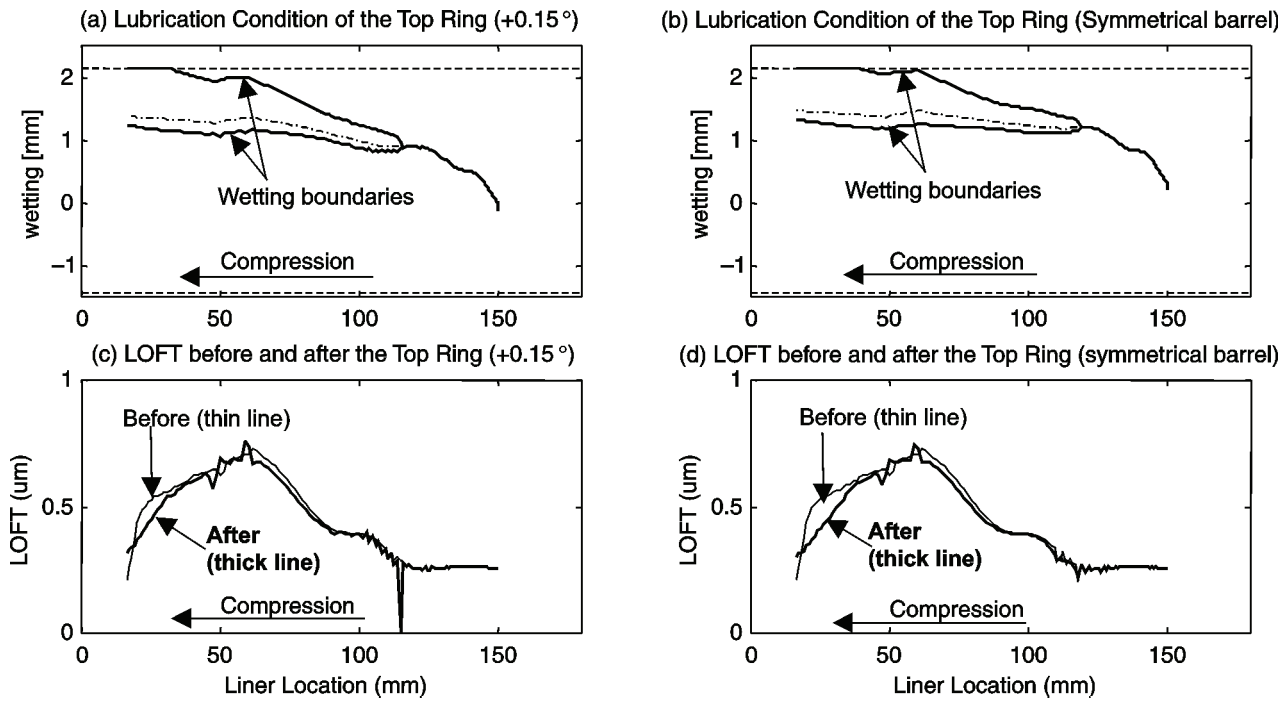

Fig. 18 Top-ring scraping with a larger groove downward tilt and a symmetrical barrel face

groove tilt angle and a symmetrical barrel profile on the running surface. The original groove tilt angle was used for the symmetrical barrel face case. Decreasing the downward groove tilt angle results in a greater concentration of the contact pressure and thus a faster increase in the downward tilt angle as the engine wears down. Conversely, using a symmetrical barrel face causes more wear at the ID of the groove and thus the groove downward tilt angle may actually decrease. Further calculation showed that, using a symmetrical barrel face, the groove downward tilt angle that gives uniform average contact pressure along the radial direction is 0.17° less than using the original offset barrel face.

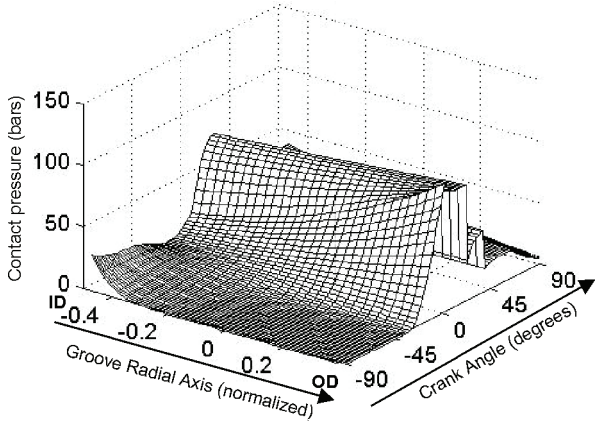

Fig. 19 Contact pressure distribution between the lower flank of the top ring and groove

6 EVOLUTION OF THE SECOND RING RUNNING SURFACE PROFILE: A PRACTICAL APPROACH

Unlike the top-ring running surface profile that usually is a design parameter, only the taper angle is specified for a taper face second ring. The profile of the lower part of the running surface is formed gradually by wear. It is of practical interests to have knowledge of the profile of the lower worn part of the taper face.

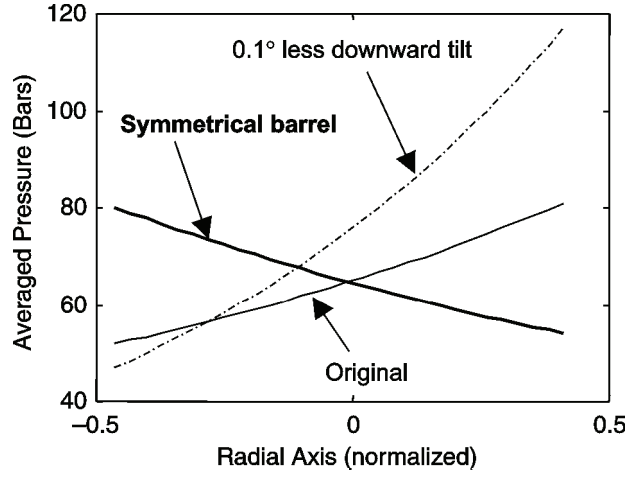

Fig. 20 Average contact pressure between the top-ring lower flank and the groove with different groove tilt angle and face profile

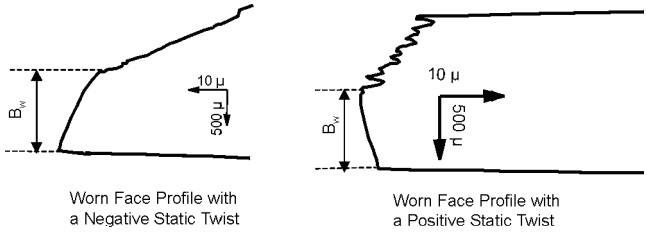

Fig. 21 Worn face profile of second rings with different static twists

As shown in Fig. 21, the worn profiles of the second ring depend on the static twist of the second ring. Here, a simple formula is given to determine the worn profile of the running surface based on the geometrical constraint from ring twist and piston tilt.

As shown in Fig. 22, assuming that the worn profile of the second ring is represented with a second-order polynomial, the coefficients of the polynomial can be obtained with the following two geometrical constraints:

1. The minimum point moves to the middle of the worn part with the ring static twist only.
2. The maximum piston tilt moves the minimum point to either the upper or lower end of the worn part.

The polynomial can be expressed as

$$h(x) = \frac{\beta}{B_w}x^2 + (\beta - \alpha_{st})x \tag{2}$$

where B_w is the axial width of the worn part, β is the maximum piston tilt angle and α_{st} is the static twist of the second ring. Certainly, when the dynamic twist of the second ring becomes significant, β in equation (2) should include the variation in the ring twist and α_{st} should be understood as the averaged ring twist.

All the results shown in this paper adapt equation (2) to determine the second ring face profile. Figure 23 shows the contact pressure on the worn part of the running surface of the second ring at the minor thrust side. It can be seen that the contact pressure spreads over the entire worn face.

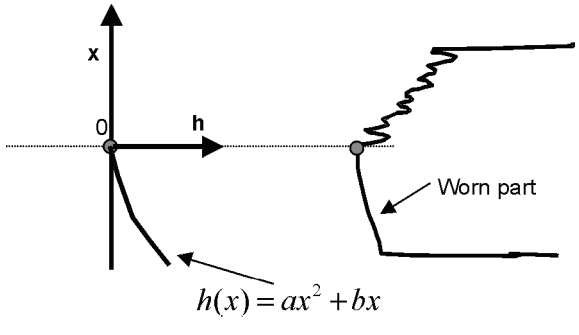

Fig. 22 Definition of the worn part profile

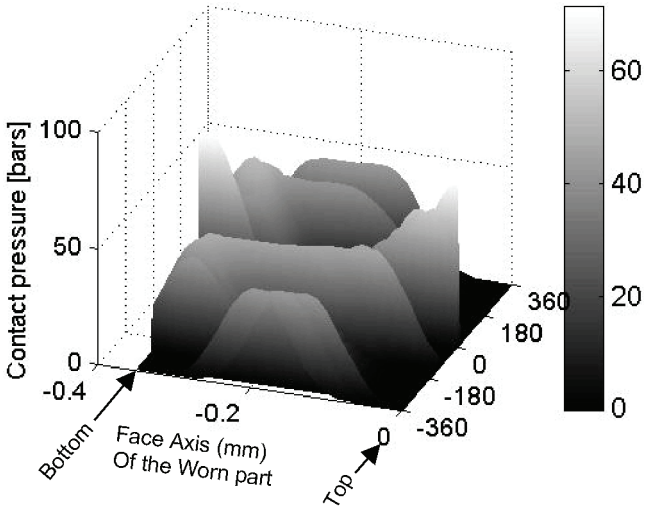

Fig. 23 Asperity contact pressure distribution on the second ring worn face

7 EFFECTS OF SURFACE ROUGHNESS ON FRICTION LOSS AND A PRACTICAL APPROACH TO ROUGHNESS TRUNCATION

Figure 24 shows the effect of liner surface roughness on the FMEP of the ring pack from different rings and different mechanisms. The results in Fig. 23 neglect the effects of piston tilt and the oil supply to the second ring during downstrokes is assumed to be sufficient (OS1). It is apparent that the roughness of the liner is critical to the friction loss of the ring pack.

In the present model, the averaged Reynolds equation given by Patir and Cheng [**18**, **19**] is used for hydrodynamic lubrication and the Greenwood–Tripp [**7**] asperity contact model [**6**] is used for boundary lubrication. As is known, the height distribution of the surface roughness in these two models is assumed to be Gassian and the only parameter that determines the roughness height distribution is the r.m.s. of the roughness distribution or R_q according to the Deutsches Institut für Normung (DIN) standard. In reality, roughness with a plateau height distribution may be used for new liners and the liner roughness becomes a plateau distribution after a short running time even when it starts with a Gaussian distribution (called a peak surface finish in practice) [**20**]. When the roughness is a plateau distribution, applying R_q from the standard measurement in the two lubrication models may overestimate the importance of the roughness effects due to the overwhelming contribution to R_q from the valley part of the roughness. Thus, as pointed out by Visscher *et al.* [**21**], the valley region needs to be excluded to reflect better the effects of surface roughness with a plateau distribution. Here, a more direct truncation method is proposed using the standard (DIN) measure-

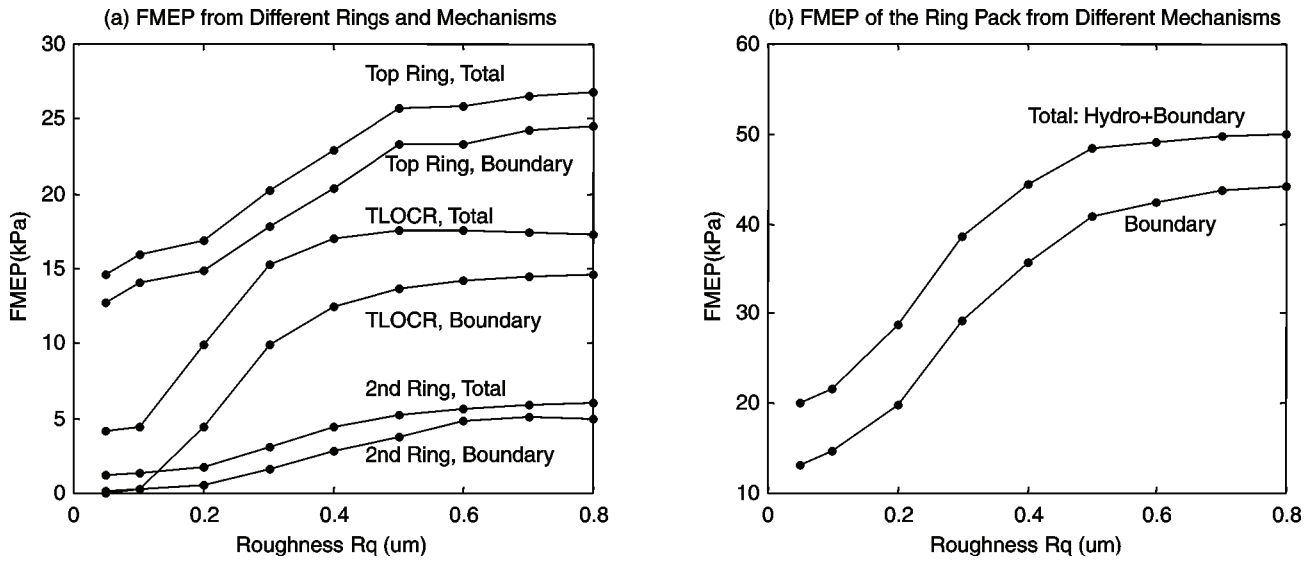

Fig. 24 Effect of liner roughness on FMEP

ment values (R_k and M_{r1}) for surface roughness. It can be seen that the present method essentially is the same as that proposed by Visscher *et al.* [**21**].

The key coordinates of a plateau roughness distribution are shown in Fig. 25 according to the definition in DIN 4776. The key assumption for the truncation is that in the core region and above there is a Gaussian distribution. Consequently, the Gaussian part of the original plateau distribution (dotted curve in Fig. 25) can be readily represented as

$$f(x) = \frac{a}{\sqrt{2\pi}\sigma} \, e^{-\frac{x^2}{(2\sigma^2)}} \tag{3}$$

where a in equation (3) should be less than 1 if the original roughness is of a plateau native. σ in equation (3) is thus R_q or the r.m.s. of the roughness distribution after the truncation. From the definition of R_k and M_{r1}

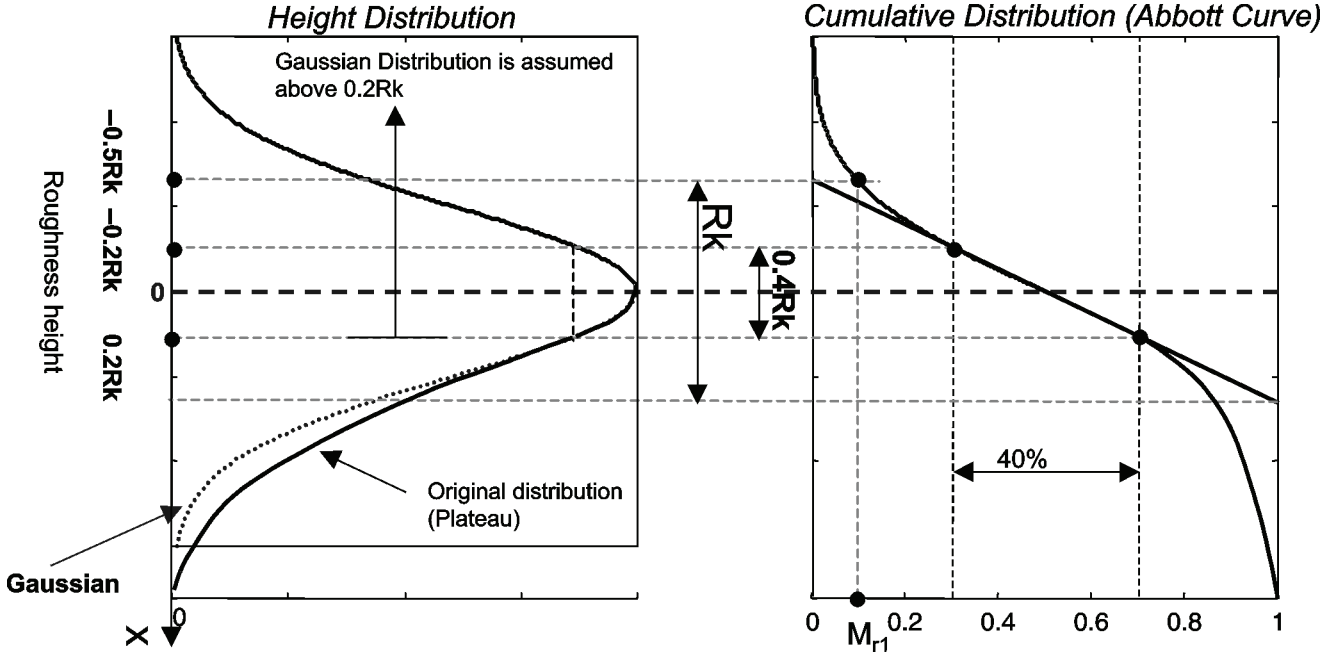

Fig. 25 Key coordinates according to DIN 4776

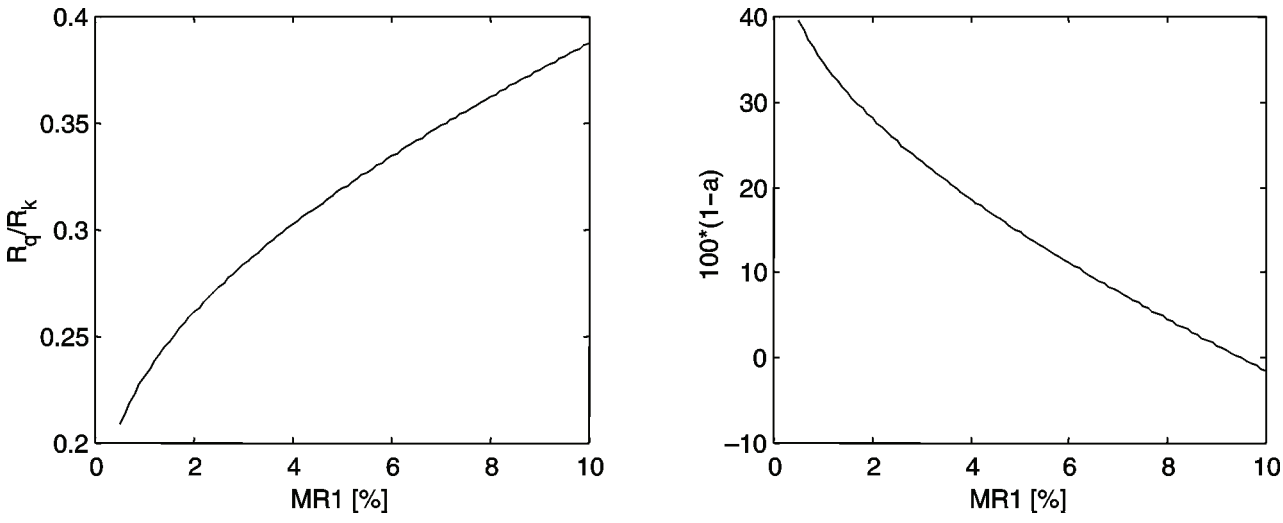

Fig. 26 Dependences of normalized R_k and percentage of the excluded roughness on M_{r1}

in DIN 4776,

$$\int_{-\infty}^{-0.5R_k} \frac{a}{\sqrt{2\pi}\sigma} e^{-\frac{x^2}{(2\sigma^2)}} dx = M_{r1}$$
$$\int_{-0.2R_k}^{0.2R_k} \frac{a}{\sqrt{2\pi}\sigma} e^{-\frac{x^2}{(2\sigma^2)}} dx = 0.4 \quad (4)$$

Solving equation (4), the truncated R_q and the percentage of the valley part that is excluded can be obtained. Furthermore, equation (4) can be reorganized as the following to obtain a more universal form by defining a new variable $\bar{R}_k$ such that $\bar{R}_k = R_k/(\sqrt{2}\sigma)$:

$$a\left(\frac{1}{2} - \frac{1}{\sqrt{\pi}} \int_0^{0.5\bar{R}_k} e^{-y^2} dy\right) = M_{r1}$$
$$\frac{a}{\sqrt{\pi}} \int_0^{0.2\bar{R}_k} e^{-y^2} dy = 0.2 \quad (5)$$

Eliminating a from equation (5), a single equation relating $\bar{R}_k$ and M_{r1} can be obtained:

$$\int_0^{0.5\bar{R}_k} e^{-y^2} dy + 5M_{r1} \int_0^{0.2\bar{R}_k} e^{-y^2} dy - \frac{\sqrt{\pi}}{2} = 0 \quad (6)$$

Figure 26 shows the dependence of the truncated $\sigma(R_q)$ and the percentage of the roughness excluded on M_{r1}, based on the results from equations (5) and (6).

8 CONCLUDING REMARKS

Using an HD diesel engine as an example, the paper first discusses the oil supply mechanisms to different liner regions and different rings and the effects of piston and piston ring dynamics. In general, the oil lubricating the ring–liner interface comes from two sources, namely from the ring–liner interaction and from the piston lands. The present paper mainly deals with the oil transport through the ring–liner interaction in the piston ring pack. Considering the oil transport mechanisms through ring–liner interaction, the liner needs to be divided into two distinctive regions, separated by the TDC location of the oil control ring. Below the TDC location of the oil control ring, the oil supply to the top two rings through ring–liner interaction is controlled by the lubrication between the OCR and the liner during downstrokes when there is sufficient oil supply to the OCR. On the other hand, above the TDC location of the OCR, called the 'dry' region in this paper, the top two rings are lubricated by the oil carried into this region by mainly the top ring. Consequently, the oil availability before the top ring enters the 'dry' region during the compression stroke and the piston dynamics are found to be the key to transporting oil to the 'dry' region via the 'carrying' ability of the top ring. The examples in this paper show that, relying solely on ring–liner interaction, it is not possible to wet the 'dry' region over all the circumference. Lack of sufficient oil supply in the 'dry' region adds another adverse effect to the list of commonly recognized causes for the severity of the top-ring–liner lubrication in HD diesel engines such as high temperature, high pressure and low piston travelling speed, and it is one of the main reasons for the large contribution of top ring to the total friction power loss of the ring pack in the HD diesel engine. Furthermore, oil transport mechanisms to the second ring and the lubrication of the second ring and liner significantly affect the oil availability to the top ring throughout the cycle and thus friction, wear and oil transport by the top ring. Ring–liner lubrication is found to be largely affected by the dynamics of the piston and rings through controlling the converging width on the running surface. Specifically, the top-ring groove tilt angle is found to be critical to the friction, wear of the top-ring running

surface and oil transport between the top ring and the liner. On the other hand, the top-ring running surface profile and the top-ring–liner lubrication affect the wear process of the top-ring groove angle. Thus, in order to optimize the top-ring groove tilt angle and top-ring running surface profile, the interaction between the ring–groove lubrication and ring–liner lubrication needs to be considered. Moreover, top-ring scraping under a high cylinder pressure is considered to be a possible main contributor to the increased oil consumption when the OCR ring is not able to conform well to the bore, which further complicates the importance of the optimization of the top-ring and groove designs.

For practical purposes, the paper also gives the equations that determine the second ring face worn profile as well as a simple truncation method for plateau liner roughness in order to utilize effectively the mixed-lubrication models based on Gaussian distribution. In summary, ring–liner lubrication is not an isolated problem and it involves such factors as the dynamics of the piston and rings, gas pressures in different regions and different mechanisms of oil supply through ring–liner interaction as well as from the piston to liner. Accurately determining the ring pack friction, oil consumption from ring–liner interaction, and wear needs resolution of all these factors. Furthermore, in reality, due to ring rotation and change in the oil distribution on the piston [**9**, **10**], engines do not necessarily produce the same results in friction and oil consumption from cycle to cycle, and wear evolution of the lubricating surfaces can affect the ring pack performance. Therefore, it is critical to understand the physics of the processes that dictate the performance of the ring–liner lubrication in order to predict it and to understand its uncertainties.

ACKNOWLEDGEMENTS

All the work presented in this paper has been sponsored by the Consortium on Lubrication in Internal Combustion Engines at Massachusetts Institute of Technology (MIT). The current consortium members are Dana Corporation, Renault SA, Peugeot PSA, Volvo AB and Mahle GmBh. The views and results in the paper are intended to reflect the physics believed to be important in ring–liner lubrication based on the evidence of engine tests on wear patterns, friction and oil-film thickness measurements conducted by MIT and the consortium members over the years. The author would like to thank Remi Rabute at Dana Corporation for our countless discussions on ring design and engine test in wide variety of engines, model applications and necessary elements to improve the models based on practical considerations. Discussions with Fredrik Stromstedt at Volvo also contributed a great deal to the content of the paper. The author would like to thank Dr Rolf-Gerhard Fiedler and Dr Eberhard Kopf at Mahle, Jonas Rick, Bengt Olson, Dr Adam Blomburg and Dr Lars Lundin at Volvo, Dr Mokhtar Maamouri at Renault, Nick Lee and Dr Bernard Cousyn at Peugeot PSA and Randy Lunsford at Dana for sharing their experience in piston ring areas, engine test results, experimental measurements and their feedback in applying the models. The author would like to thank Dr Benoist Thirouard, Ertan Yilmaz, Dr Victor Wong and Professor Heywood at MIT for all the helpful discussions over the years.

REFERENCES

1 **Tian, T.** Modeling the performance of the piston ring pack in internal combustion engines. PhD thesis, Department of Mechanical Engineering, Massachusetts Institute of Technology, June 1997.

2 **Tian, T., Wong, V. W.** and **Heywood, J. B.** A piston ring-pack film thickness and friction model for multigrade oils and rough surfaces. SAE paper 962032, 1996; also in *SAE Trans. J. Fuels Lubricants*, 1996, **105**(4), 1783–1795.

3 **Tian, T., Noordzij, L. B., Wong, V. W.** and **Heywood, J. B.** Modeling piston-ring dynamics, blowby, and ring-twist effects. *Trans. ASME, J. Engng Gas Turbines Power*, 1998, **120**(4), 843–854.

4 **Rabute, R.** and **Tian, T.** Challenges involved in piston top ring designs for modern SI engines. *Trans. ASME, J. Engng Gas Turbines Power*, 2001, **123**(2), 448–459.

5 **Tian, T.** Dynamic behaviours of piston rings and their practical impact. Part I: ring flutter and ring collapse and their effects on gas flow and oil transport. *Proc. Instn Mech. Engrs, Part J, J. Engineering Tribology*, 2002, **216**, 209–228.

6 **Hu, Y., Cheng, H. S., Arai, T., Kobayashi, Y.** and **Aoyama, S.** Numerical simulation of piston ring in mixed lubrication—a nonaxisymmetrical analysis. *Trans. ASME, J. Tribology*, 1994, **116**, 470–478.

7 **Greenwood, J. A.** and **Tripp, J. H.** The contact of two nominally flat surfaces. *Proc. Instn Mech. Engrs*, 1971, **185**, 625–633.

8 **Richardson, D. E.** and **Krause, S. A.** Predicted effects of cylinder kit wear on blowby and oil consumption for two diesel engines. *Trans. ASME, J. Engng Gas Turbines Power*, 2000, **122**, 520–525.

9 **Thirouard, B.** Characterization and modeling of the fundamental aspects of oil transport in the piston ring pack of internal combustion engines. PhD thesis Department of Mechanical Engineering, Massachusetts Institute of Technology, June 2001.

10 **Thirouard, B., Tian, T.** and **Hart, D. P.** Investigation of oil transport mechanisms in the piston ring pack of a single cylinder diesel engine, using two dimensional laser induced fluorescence. Presented at SAE Fall Fuels and Lubricants Meeting and Exposition, October 1998, San Francisco, California: also in *SAE Trans., J. Fuels Lubricants*, 1998, **107**, 2007–2015.

11 **Noordzij, L. B.** Measurement and analysis of piston inter-ring pressures and oil-film thickness and their effects on

engine oil consumption. MS thesis, Department of Mechanical Engineering, Massachusetts Institute of Technology, June 1996.

12 **Piao, Y.** and **Gulwadi, S. D.** Effect of piston secondary motion on the numerical modeling of the piston ring pack performance. Proceedings of the 2000 Full Technical Conference of the ASME ICE Division, vol. 35-3, pp. 51–59.

13 **Casey, S.** Analysis of lubricant film thickness and distribution along the piston/ring/liner interface in a reciprocating engine. MS thesis, Department of Mechanical Engineering, Massachusetts Institute of Technology, February 1998.

14 **Tian, T.** and **Wong, V. W.** Modeling the lubrication, dynamics, and effects of piston dynamic tilt of twin-land oil control rings in IC engines. *Trans. ASME, J. Engng Gas Turbines Power*, January 2000, **122**, 119–129.

15 **Carrié, O.** and **Maerky, C.** U-flex as an oil control ring for new generation engines. *Motortechnische Z.*, 1999, **60**, 570–575.

16 **Tian, T., Rabute, R., Wong, V. W.** and **Heywood, J. B.** Effects of piston-ring dynamics on ring/groove wear and oil consumption. SAE paper 970835, 1997; also presented at SAE International Congress and Exposition, Detroit, Michigan, February 1997; also in *SAE Trans., J. Engines*, 1997, **106**, 1195–1207.

17 **Piao, Y.** and **Gulwadi, S. D.** Effect of piston secondary motion on the numerical modeling of the piston ring pack performance. Presented at ASME ICE Division 2000 Fall Technical Conference, 24–27 September 2000, Peoria, Illinois.

18 **Patir, N.** and **Cheng, H. S.** An average flow model for determining the effects of three-dimensional roughness on partial hydrodynamic lubrication. *Trans. ASME, J. Lubric. Technol.*, 1978, **100**(1), 12–17.

19 **Patir, N.** and **Cheng, H. S.** Application of average flow model to lubrication between rough sliding surfaces. *Trans. ASME, J. Lubric. Technol.*, 1979, **101**, 220–230.

20 **Hill, S. H., Kantola, T. C., Brown, J. R.** and **Hamelink, J. C.** An experimental study of the effect of cylinder bore finish on engine oil consumption. SAE paper 950938, 1995.

21 **Visscher, M., Downson, D.** and **Taylor, C. M.** Surface roughness modeling for piston ring lubrication: solving the problems. In *The Third Body Concept: Interpretation of Tribological Phenomena*, Proceedings of the 22nd Leeds–Lyon Symposium on *Tribology*, Lyon, September 1995, 1996 (Elsevier, Amsterdam) pp. 527–537.